Mineralogical Magazine, June 1998, Vol. 62(3), pp. 421–429

Tungsten-bearing rutile from the Kori Kollo gold mine, Bolivia

C. M. RICE, K. E. DARKE, J. W. STILL

Department of Geology and Petroleum Geology, University of Aberdeen, Aberdeen, Scotland

AND

E. E. LACHOWSKI

Department of Chemistry, University of Aberdeen, Aberdeen, Scotland

ABSTRACT

W-bearing rutile formed during alteration of jarosite by resurgent hydrothermal fluids in the oxide zone of the Kori Kollo gold deposit. The rutile shows sector zoning in basal sections and well developed multiple growth zones, both defined in backscatter electron images by variations in the W content. The maximum WO_3 content is 5.3 wt.% and W substitutes for Ti with double substitution of Fe to maintain charge balance. The causes of multiple growth bands are considered to be changes in externally controlled variables occurring in a shallow hydrothermal system. Whereas Ti is probably leached from biotite in dacitic rocks, the W is introduced by hydrothermal fluids.

KEYWORDS: tungsten, rutile, jarosite, gold deposits, Bolivia.

Introduction

TUNGSTEN-BEARING rutile is a rare occurrence. Standard mineral reference texts discuss the common substitution of Fe, Nb, Al, Ta, Sn and Cr into the rutile structure, but there is no reference to tungsten. The first mention of W in rutile was at Big Bell, Western Australia, where it occurs in mica schist and pegmatite. The rutile contains up to 5.8 wt.% WO_3 and also 1.7 wt.% Sb_2O_5 and 1.7 wt.% FeO (Graham and Morris, 1973).

Two further occurrences of W-bearing rutile have been reported. In the Hemlo gold deposit, Ontario, Canada (Harris, 1986) rutile occurs in pyritic ore together with barite and molybdenite. It contains up to 2.3 wt.% WO_3, 5.6 wt.% V_2O_3 and 6.5 wt.% Sb_2O_5. Rutile with up to 7.2 wt.% WO_3 and 16.8 wt.% Nb_2O_5 is found in a metasomatised molybdenite-bearing aplite from N.Greece (Michailidis, 1997).

This study reports a well characterised W-bearing rutile showing multiple growth and sector zoning from a hydrothermal alteration zone at the Kori Kollo gold mine, Bolivia.

Geological setting

Kori Kollo is the largest gold mine in Bolivia, and is a precious-metal-rich variety of the polymetallic vein deposits characteristic of the Bolivian Altiplano (Ludington *et al.*, 1992). It is located within one of a cluster of altered dacitic stocks of Miocene age in the La Joya District 40 km west of Oruro, Bolivia (Columba and Cunningham, 1993). The country rocks consist of silts and shales of the Silurian Catavi formation. The Kori Kollo stock comprises three phases of dacite, varying from fine to coarse grained, with feldspars, biotite and quartz phenocrysts. Feldspar and biotite are altered to sericite and the groundmass is a mixture of sericite and quartz.

Mineralisation occurs in parallel fractures related to a regional shear zone. The fractures are filled with an assemblage of sulfides, consisting of early pyrite, trace arsenopyrite and chalcopyrite, and late stage sulfides and sulfosalts in the centre of the veins. Gold occurs as submicron gold within early disseminated pyrite, and associated with the late mineralisation. An oxidation zone, composed of iron oxides, jarosite

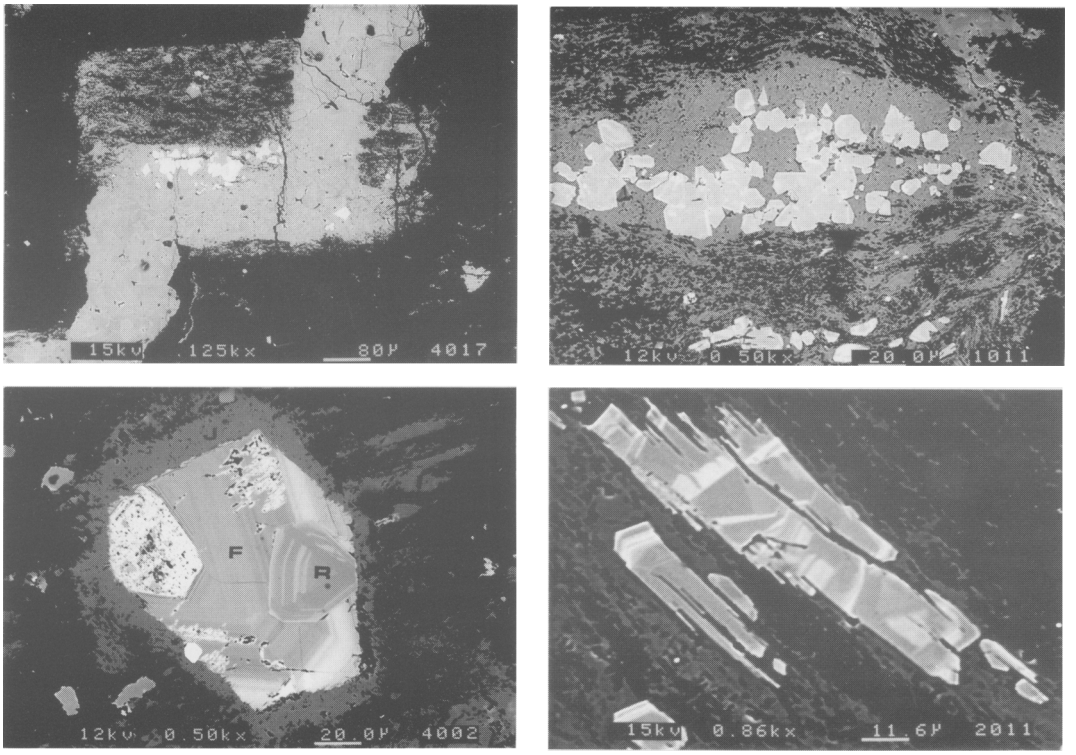

FIGS 1–4. Fig. 1. (*top left*) Rectangular biotite crystal cut by jarosite vein. Biotite is altered to quartz (black) and jarosite (medium grey). Jarosite vein contains clusters of rutile crystals (white) where cutting the biotite. BSEI. Fig. 2. (*top right*) Subhedral rutile crystals (white) replacing lens of jarosite within biotite. Note development of irregular elongated rutile crystals (bottom of figure) where the proportion of jarosite decreases. BSEI. Fig. 3. (*lower left*) Rutile (R) mantled by florencite (F) showing multiple zoning which, in turn is mantled by jarosite (J). The florencite core is *REE* rich. Black areas are quartz. BSEI. Fig. 4. (*lower right*) Rutile crystals selectively replacing lenses of jarosite (medium grey). Growth of rutile is limited by intervening lenses of quartz (black). Rutile shows complex multiple growth and sector zoning. Euhedral faces only occur along the jarosite replacement front. W rich zones are white. BSEI.

and alunite, forms a 40–70 m thick capping on the dacite.

Altered dacites from Kori Kollo contain anomalous quantities of W (c. 55 ppm), which indicates similarities to the nearby La Joya dacite stock where W-bearing gold veins have been reported (Redwood, 1986), and a sample of this dacite contains 430 ppm W. Tungsten enrichment is common in Bolivian polymetallic vein deposits, and W-bearing rutile may not be restricted to Kori Kollo.

Paragenesis and zoning

The W-bearing rutile is found within the oxidation zone in altered phenocrysts of biotite (commonly 0.5–1.5 mm) or in jarosite veins cutting biotite (Figs 1,2). Alteration consists of various combinations of quartz and jarosite with a strong linear fabric, probably related to the original sheet structure of the biotite. Rutile preferentially replaces jarosite and occurs either as individual red-brown subidiomorphic crystals up to 60 µm along the maximum dimension or aggregates of crystals, frequently intergrown (Fig. 2). The rutile is postdated by florencite and further jarosite (Fig. 3). Florencite and other phosphates such as hinsdalite are common at Kori Kollo and are closely associated with the sulphates, jarosite and alunite, in the oxide zone (Darke, 1997).

Individual crystals may show complex habits which are partly controlled by the shape of the

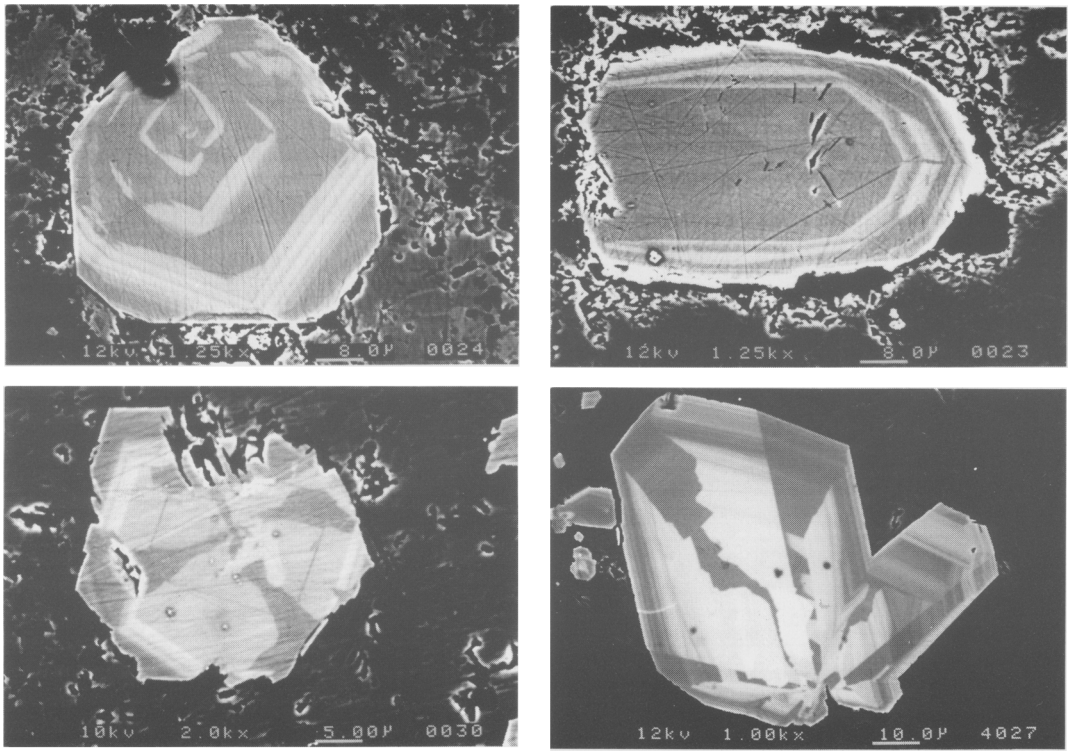

FIGS 5–8. Fig. 5. (*top left*) Basal section of rutile showing two episodes of oscillatory zoning. Early wide zones followed by later narrow ones. Early growth followed one prism form whereas the latest phase (current crystal growth surface) is following two prism forms. Fig. 6. (*top right*) Prismatic rutile showing two pyramid forms. Core shows continuous growth followed by multiple discontinuous zones. BSEI. Fig. 7. (*lower left*) Basal section of rutile crystal showing well developed early sector zoning under two prism forms (W-rich sectors are white) followed by multiple growth zoning. BSEI. Fig. 8. (*lower right*) Oblique basal section of rutile showing sector zoning and fine scale (submicron) discontinuous zoning. Early zones are W rich. BSEI.

jarosite aggregates being replaced (Fig. 4). Crystal faces are best developed, and growth preferentially proceeds, where the replacement front is largely or entirely composed of jarosite (Figs 2, 4). The faces comprise two prism and two pyramid forms which are variably developed (Figs 5,6). We have not been able to index these forms (see below) but they probably include the main rutile forms {100} {110} and {111} or {101}. Sometimes the prism forms change during the growth of individual crystals (Fig. 5).

Many crystals show well developed multiple growth and sector zoning using backscatter electron imagery (BSEI) (e.g. Figs 5,6,7) which is largely due to variations in the W content (see composition). BSEI is a particularly sensitive technique in this case because of the large difference between the atomic numbers of W and the other cations. The growth zones comprise discontinuous, oscillatory and convolute varieties (Mackenzie *et al.*, 1982). Discontinuous zones show variable widths on the sub-micron to micron scale and a range of W contents, as judged by BSEI (Fig. 8), whereas in oscillatory zoning the widths are more uniform and the W content displays regular variations (Fig. 5). Both zone types may occur in the same crystal (Figs 9, 10). Convolute zones are sinuous and individual zones may show variable thickness on a face and be restricted to that face (Fig. 9). Sector zoning is only seen in basal sections with two prism forms where the composition planes radiate from a central point (Fig. 7). The zones are distinguished on the basis of their W content which represents

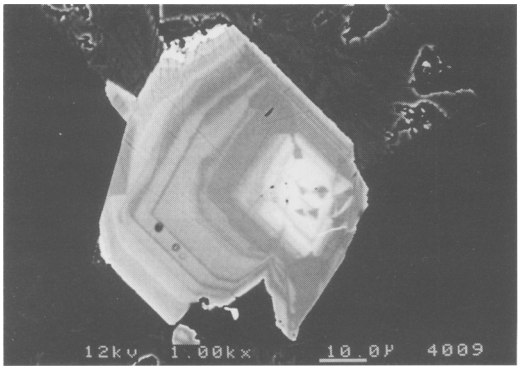

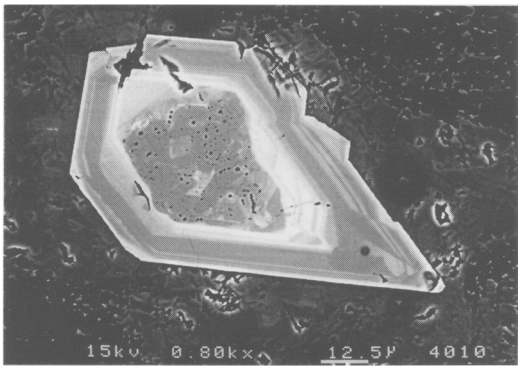

FIGS. 9 and 10. Fig. 9. (*left*) Basal section of rutile showing multiple discontinuous, oscillatory and convolute zoning. Early growth zones are W rich. Growth has largely proceeded under one prism form. BSEI. Fig. 10. (*right*) Distorted basal section of rutile showing corroded spongy core (note relict jarosite textures) mantled by multiple discontinuous and oscillatory zones. Early zones are W-rich. BSEI.

differential incorporation of W under the two prism zone forms. An attempt to index these prism forms using a beam tilting device on an SEM failed as the electron beam destroyed the crystal. Sometimes crystal cores lack multiple growth zones and record an early period of relatively uniform isochemical growth (in terms of W content) (Figs 6,7). These cores may be corroded and spongy (Fig. 10). Later growth is characterised by multiple growth zones which mantle the cores (Figs 7,10,11). In some cases the growth zoning displays a stratigraphy that can be traced from crystal to crystal (Fig. 11, compare also Figs 9,10).

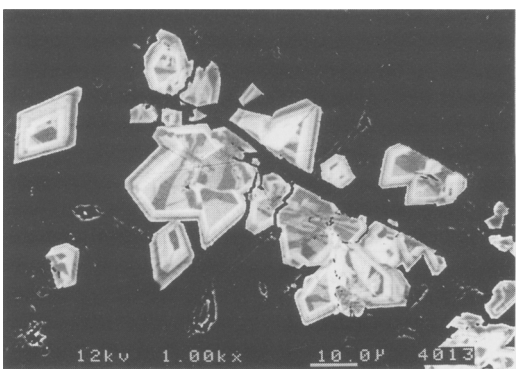

FIG. 11. Cluster of rutile crystals showing early sector zoning followed by multiple zoning. The stratigraphy of the latter zoning is similar between crystals and also similar to Fig. 7. BSEI.

Composition

Five rutile crystals were analysed by EPMA (Table 1). In three crystals the discontinuous zones with minimum and maximum W content, as distinguished by BSEI were analysed. In the fourth and fifth crystals the two types of sector zone and spongy core, respectively, were analysed. The cation totals are close to one per unit cell indicating that the oxidation states for the cations are essentially correct. Overall the W levels range from 0.1 to 5.3 wt.% WO_3. Small amounts of Fe, Nb, Al and Cr were also detected but no Sb (det. limit 0.02%). The maximum Fe content (2 mole %)is close to the limit of substitution (1 mole %) seen in artificial (formed at <1000°C) and natural rutiles (Rumble, 1976; Vlassopoulos *et al.*, 1993; Wittke, 1967). Numerous studies of the oxidation state of iron in synthetic rutile (see Vlassopoulos, 1993, for a review) and natural rutile (Murad *et al.*, 1995) indicate that iron is mainly present as Fe^{3+} in the Ti site. With the exception of W and to a lesser extent Fe there is little difference in composition between the sector zones. W and Fe atoms are concentrated in one of the two sector forms by factors of about 20 and 3, respectively.

Crystal structure

Analytical transmission electron microscopy studies (Jeol 2000EX Temscan) of an argon-milled section confirm that the TiO_2 polymorph is

TABLE 1A: Composition of growth zones with maximum and minimum W-content in three rutile crystals

Crystal	KK1A				KK1B				KK1C			
% Oxide		formula		formula		formula		formula		formula		formula
TiO_2	94.7	0.972	96.6	0.982	94.6	0.968	97.5	0.984	92.3	0.950	98.5	0.983
WO_3	2.2	0.008	0.3	0.001	3.3	0.012	0.5	0.002	4.6	0.017	0.2	0.001
Fe_2O_3	1.3	0.014	0.7	0.007	1.1	0.012	0.9	0.009	2.0	0.021	1.2	0.012
Nb_2O_5	0.3	0.002	0.2	0.001	0.4	0.002	0.1	0.001	0.7	0.004	0.3	0.002
Al_2O_3	0.2	0.003	0.5	0.008	0.1	0.002	0.2	0.003	0.2	0.003	0.3	0.004
Cr_2O_3	0.1	0.001	0.2	0.002	0.0	0.000	0.1	0.001	0.1	0.001	0.1	0.001
Total	98.8	1.000	98.5	1.001	99.5	0.996	99.3	1.000	99.9	0.996	100.6	1.003

TABLE 1B. Composition of sector zones in one rutile crystal

% Oxide	1	formula	2	formula	3	formula	4	formula
TiO_2	92.3	0.949	94.6	0.964	98.4	0.990	98.1	0.990
WO_3	5.3	0.019	3.4	0.012	0.2	0.001	0.1	0.000
Fe_2O_3	1.9	0.020	1.6	0.016	0.6	0.006	0.6	0.006
Nb_2O_5	0.4	0.003	0.3	0.002	0.1	0.001	0.1	0.001
Al_2O_3	0.2	0.004	0.2	0.003	0.1	0.002	0.2	0.002
Cr_2O_3	0.1	0.001	0.1	0.001	0.2	0.002	0.1	0.001
Total	100.2	0.996	100.2	0.998	99.6	1.002	99.2	1.000

TABLE 1C. Composition of spongy core in one rutile crystal

% Oxide		formula		formula
TiO_2	98.1	0.985	96.5	0.976
WO_3	0.3	0.001	1.5	0.005
Fe_2O_3	0.9	0.009	1.1	0.011
Nb_2O_5	0.2	0.001	0.2	0.001
Al_2O_3	0.2	0.003	0.3	0.004
Cr_2O_3	0.0	0.000	0.1	0.001
Total	99.7	0.999	99.7	0.998

Table 1B: Analyses 1 and 2 correspond to high W zones as defined by a backscattered electron image and 3 and 4 are low W zones
Table 1C: Analyses chosen to reflect variation in W content.
Wavelength dispersive analyses by Cambridge Scientific Instruments MICRO SCAN MK5 (Link Analytical ZAF4/FLS program used for ZAF corrections)
Analyst: J. W. Still, Department of Geology, Aberdeen University.

rutile. Energy-dispersive X-ray analysis (Link 10/85S) was used to locate a TiO_2 crystal and its unit cell was determined by selected area electron diffraction. Figure 12 shows the [010] zone axis. The unit cell dimensions were found to be a 4.60 and c 2.94 Å, in good agreement with the values for rutile, and tilting experiments showed that the observed diffraction spots were consistent with the appropriate space group, $P4_2/mmm$ (ref. National Bureau of Standards Monograph 25, Sect. 7, 1969).

Discussion

Location of W and substitution mechanisms

Fe, Nb, Al and Cr show a strong inverse correlation with Ti (r = −0.916) (Fig. 13A), consistent with ionic substitution, as reported by previous workers (Deer *et al.*, 1992). Inclusion of W produces an improved correlation (r = −0.993) suggesting a similar mechanism for this cation (Fig. 13B). A location in mineral inclusions is unlikely since, apart from jarosite and quartz, no inclusions were observed in the rutile either by optical or BSEI studies. The radii of the likely ions for these five metals (eg. W^{6+}, Nb^{5+}, Ti^{4+}, Al^{3+}, Cr^{3+}, Fe^{3+}) are similar, but the charge variations would require additional substitutions to maintain electrical neutrality. The substitution of Ti in rutile by significant quantities of overcharged ions such as Nb and Ta is well known (e.g. Deer *et al.*, 1992) and more recently rutiles with up to 33.75 wt% Sb_2O_5 have been reported (Smith and Perseil, 1997). In these examples Fe is also present in major amounts which suggests that double substitutions of the kind $2Ti^{4+} \rightarrow Fe^{3+} + M^{5+}$, or possibly $3Ti^{4+} \rightarrow Fe^{2+} + 2M^{5+}$ have occurred. In Kori Kollo rutiles with high W levels the number of W and Fe atoms in the formula is roughly equal, also suggesting a double substitution mechanism: $2Ti^{4+} \rightarrow Fe^{3+} + W^{6+}$. The excess positive

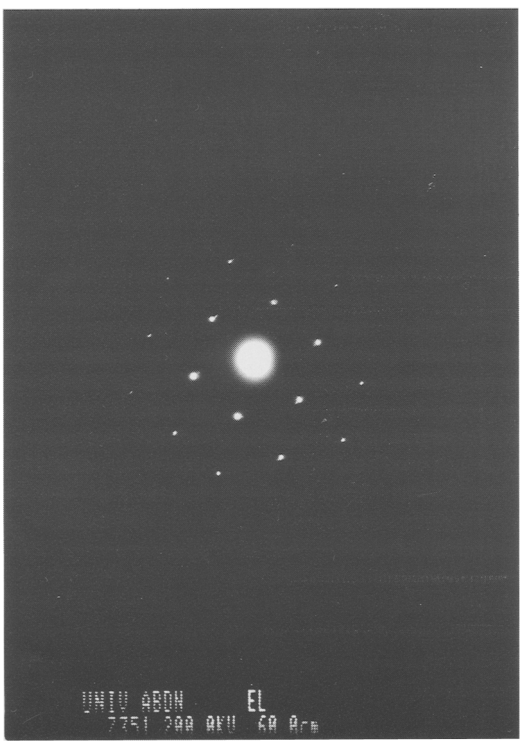

FIG 12. Electron diffraction pattern of rutile [010] axis.

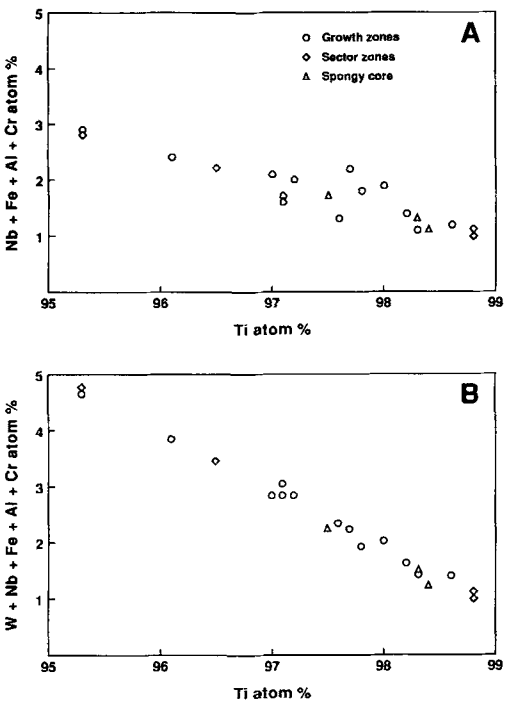

FIG. 13(A) Plot of Ti against Fe, Nb, Al and Cr (atom % per formula unit) shows a strong inverse correlation (r = −0.916) consistent with substitution for Ti in the rutile structure. (B) The inclusion of W produces a stronger correlation (r = −0.993) indicating that W also substitutes for Ti. Data include analyses of other crystals not reported in Table 1.

charge could be balanced by vacancies in the Ti sites or by loss of oxygen as a gas. The electrons so released would remain in the structure to compensate the positive charge (Tilley, 1987). It is also possible that in this rutile Fe is present in the reduced state and the mechanism is $2Ti^{4+} \rightarrow Fe^{2+} + W^{6+}$

Causes of sector zoning

Sector zoning has been reported in a number of minerals including clinopyroxene, calcite and titanite (e.g. Larsen, 1981; Reeder and Paquette, 1989; Paterson *et al.*, 1989; Bouch *et al.*, 1997) but not, so far, in rutile. It is generally understood to reflect disequilibrium at the crystal-growth surface and sector zones result when the different growth forms incorporate different quantities of impurity elements. Preservation of sector zoning then depends on the cation diffusion rate in the crystal being slower than the growth rate of that crystal (Nakamura, 1973). Various specific factors have been identified which explain the initial anisotropic enrichment and these include (1) differences in the atomic configuration of the surface on different faces (Nakamura, 1973; Dowty, 1976), (2) differences in growth rates on different faces (Downes, 1974; Larsen, 1981), (3) differences in growth mechanisms on different faces (Kouchi *et al.*, 1983) and (4) differences in face normal diffusion rates on different faces (Watson and Liang, 1995). These factors cannot be properly evaluated in the case of the Kori Kollo rutiles since we have not been able to index the prism faces. However, factor 2 is not applicable since the growth rates of the two prism forms were broadly similar (Fig. 7). W^{6+} is the most highly charged cation in the rutile and also one of the smallest and so, given that anisotropic surface enrichment of W^{6+} occurred (factors 1 and 3), it would seem likely that its anticipated slow diffusion rate compared to the other cations was a contributing factor. It is also worth noting that cation sites on the surfaces of the common prism forms {100} and {110} are different, which might provide an explanation for the sector zoning. Thus on {100} the sites have 3 out of 6 completed bonds in the first coordination sphere whereas on {110} there are sites with 4 or 5 completed bonds. According to Dowty (1977) sites with 3/6 coordinations are most likely to retain impurities and so we suggest that the W cations are being preferentially incorporated on {100}.

Causes of discontinuous, oscillatory and convolute growth zones

Most of the discontinuous growth bands are of variable width and W content. These sudden changes in composition are probably caused by changes in externally controlled variables since there are similarities in zone stratigraphy between different crystals (Figs 7, 11) (Yardley *et al.*, 1991). These variables could include changes in fluid chemistry and/or abrupt changes in pressure or temperature which would affect solid solution between Ti and W and the other cations. Such changes, together with changes in fluid supply, could also cause periods of dissolution and non-deposition. All of these changes would be expected in a shallow, open hydrothermal system such as occurred at Kori Kollo and they provide the most obvious explanation for the discontinuous growth zones.

Oscillatory zoning has been explained in terms of internal factors which result in local disequilibrium between an individual crystal and the adjacent fluid (Haase *et al.*, 1980; Allegre *et al.*, 1981; Loomis, 1982; Ortoleva *et al.*, 1987; Reeder *et al.*, 1990). However, the occurrence of discontinuous and oscillatory zoning patterns in the same crystal and the matching of these patterns between crystals (Figs 9, 10) suggests that external controls might account for both types of zoning. One possibility is the release of W-bearing hydrothermal fluids in pulses from a crystallising granitic magma (Halls, 1987), which at times might be sufficiently regular in composition and timing to generate the oscillatory zoning.

The origin of the convolute zoning is unclear. Corrosion is unlikely as it does not occur on all faces for a particular zone. It may be linked to growth problems caused by the anisotropic distribution of quartz and jarosite in the material that is being replaced (Blackerby, 1968).

Paragenesis of the rutile and source of tungsten

Rutile clearly replaces jarosite which, in turn, replaces biotite. The close spatial association between rutile and biotite strongly suggests that the original source of the Ti was biotite, which is commonly enriched in this element. The presence of jarosite predating rutile is of some interest since the former is commonly a weathering product of sulphides and a weathering origin for the jarosite at Kori Kollo is supported by stable isotope studies (Darke, 1997). Rutile is postdated by florencite and further jarosite. On the reason-

able assumption that the rutile is hydrothermal, it is clear that resurgent hydrothermal activity has invaded the weathering zone of an earlier phase of sulphide mineralisation.

Thus, the formation of W-bearing rutile is a relatively late hydrothermal event at Kori Kollo and may be connected with the formation of W-bearing gold veins which cut altered dacite of the nearby La Joya stock (Redwood, 1986). The growth history of the rutile has clearly indicated the complex nature of the hydrothermal history and underlines the importance of accessory minerals in petrogenetic studies.

Acknowledgements

This work arose from a PhD study funded by Aberdeen University. The Bolivian Mining consultancy, MINTEC, gave substantial field support. Thanks to Battle Mountain Gold and Inti Raymi for access to and sampling of Kori Kollo.

References

Allegre, C.J., Provost, A. and Jaupart, C. (1981) Oscillatory zoning: A pathological case of crystal growth. *Nature*, **294**, 223–8.

Blackerby, B.A. (1968) Convolute zoning of plagioclase phenocrysts in Miocene volcanics from the western Santa Monica Mountains, California. *Amer. Mineral.*, **53**, 954–62.

Bouch, J.E., Hole, M.J. and Trewin, N.H. (1997) Rare earth and high field strength element partitioning behaviour in diagenetically precipitated titanites. *Neues Jahrb. Mineral. Mh.*, 3–21.

Columba, M.C. and Cunningham, C.G. (1993) Geological model for the mineral deposits of the La Joya district, Oruro, Bolivia. *Econ. Geol.*, **88**, 701–8.

Darke, K.E. (1997) *Supergene mineralisation in gold-rich Bolivian polymetallic vein deposits.* PhD thesis, University of Aberdeen.

Deer, W.A., Howie, R.A. and Zussman, J. (1992) *An Introduction to Rock-forming Minerals.* Longmans Scientific & Technical, 696 pp.

Downes, M.J. (1974) Sector and oscillatory zoning in calcic augites from Mt. Etna, Sicily. *Contrib. Mineral. Petrol.*, **47**, 187–96.

Dowty, E. (1976) Crystal structure and crystal growth II: Sector zoning in minerals. *Amer. Mineral.*, **61**, 460–9.

Graham. J. and Morris, R.C. (1973) Tungsten- and antimony-substituted rutile. *Mineral. Mag.*, **39**, 470–3.

Haase, C.S., Chadam, J., Feinn, D. and Ortoleva, P. (1980) Oscillatory zoning in plagioclase feldspar, *Science*, **209**, 272–4.

Harris, D.C. (1986) Mineralogy and Geochemistry of the main Hemlo Gold Deposit, Hemlo, Ontario, Canada. *Proceedings of Gold 1986 Symposium, Toronto*, 297–310.

Halls, C. (1987) A mechanistic approach to the paragenetic interpretation of mineral lodes in Cornwall. *Proc. Ussher Society*, **6**, 548–54.

Kouchi, A., Sugawara, Y., Kashima, K. and Sunagawa, I. (1983) Laboratory growth of sector zoned clinopyroxenes in the system Ca Mg Si_2O_6 – Ca Ti Al_2O_6. *Contrib. Mineral. Petrol.*, **83**, 177–84.

Larsen, L.M. (1981) Sector zoned aegerine from the Ilimaussaq alkaline intrusion, South Greenland. *Contrib. Mineral. Petrol.*, **76**, 285–91.

Loomis, T.P (1982) Numerical simulation of crystallisation processes of plagioclase in complex melts: the origin of major and oscillatory zoning in plagioclase. *Contrib. Mineral. Petrol.*, **81**, 219–29.

Ludington, S., Orris, G.J., Cox, D.P., Long, K.R. and Asher-Bolinder, S. (1992) Mineral deposit models. *U.S.G.S Bulletin* 1975, *Geology and mineral resources of the Altiplano and Cordillera Occidental, Bolivia,* 63–90.

Mackenzie, W.S., Donaldson, C.H. and Guilford, C. (1982) *Atlas of Igneous Rocks and their Textures.* Longman. 148 pp.

Michailidis, K.M. (1997) An EPMA and SEM study of niobian-tungstenian rutile from the Fanos aplitic granite, Central Macedonia, Northern Greece. *Neues Jahrb. Mineral. Mh.*, 549–63.

Murad, E., Cashion, J.D., Noble, C.J. and Pilbrow, J.R. (1995) The chemical state of Fe in rutile from an albitite in Norway. *Mineral. Mag.*, **59**, 557–60.

Nakamura, Y. (1973) Origin of sector zoning in igneous clinopyroxenes. *Amer. Mineral.*, **58**, 986–90.

Ortoleva, P., Merino, E., Moore, C. and Chadam, J. (1987) Geochemical self-organisation I: Reaction-transport feedbacks and modelling approach. *Amer. J. Sci.*, **287**, 979–1007.

Paterson, B.A., Stephens, W.E. and Heard, D.A. (1989) Zoning in granitoid accessory minerals as revealed by back scattered electron imagery. *Mineral. Mag.*, **53**, 55–61.

Redwood, S.D. (1986) *Epithermal precious and base metal mineralisation and related magmatism on the northern Altiplano, Bolivia,* PhD thesis, Aberdeen University.

Reeder, R.J. and Paquette, J. (1989) Sector zoning in natural and synthetic calcites. *Sed. Geol.*, **65**, 239–47.

Reeder, R.J., Fagioli, R.O. and Myers, W.J. (1990) Oscillatory zoning of Mn in solution-grown calcite

crystals. *Earth Sci. Rev.*, **29**, 39–46.

Rumble, D. III (1976) In: *Oxide Minerals* (Rumble, D III, ed). Min. Soc. of America, Reviews in Mineralogy, **3**, R1–R24.

Smith, D.C. and Perseil, E.A. (1997) Sb-rich rutile in the manganese concentrations at St Marcel-Praborna, Aosta Valley, Italy: petrology and crystal-chemistry. *Mineral. Mag.*, **61**, 655–69.

Tilley, R.J.D. (1987) *Defect Crystal Chemistry and its Applications*. Blackie. 236 pp.

Vlassopoulos, D., Rossman, G.R. and Haggerty, S.E. (1993) Coupled substitution of H and minor elements in rutile and the implications of high OH contents in Nb- and Cr-rich rutile from the upper mantle. *Amer. Mineral.*, **78**, 1181–91.

Watson, E.B. and Liang, Y. (1995) A simple model for sector zoning in slowly grown crystals: Implications for growth rate and lattice diffusion, with emphasis on accessory minerals in crustal rocks. *Amer. Mineral.*, **80**, 1179–87.

Wittke, J.P. (1967) Solubility of iron in TiO_2 (Rutile) *J. Amer. Ceram. Soc.*, **50**, 586–8.

Yardley, B.W.D., Rochelle, C.A., Barnicoat, A.C. and Lloyd, G.E. (1991) Oscillatory zoning in metamorphic minerals: an indicator of infiltration metasomatism. *Mineral. Mag.*, **55**, 357–65.

[*Manuscript received 5 August 1996: revised 28 November 1997*]